Online ISSN 1848-3380, Print ISSN 0005-1144
ATKAFF 54(3), 308–315(2013)

Marek Pástor, Jaroslav Dudrik

Predictive Current Control of Grid-tied Cascade H-bridge Inverter

DOI 10.7305/automatika.54-3.186
UDK 681.518.25.013:621.314.54.072(621.383.51)
IFAC 4.3.1; 5.5.4

Original scientific paper

This paper presents a grid-tied cascade H-bridge inverter with predictive current control technique. The proposed 15-level cascade inverter consists of three H-bridge inverters with separated DC sources. At the output of the cascade inverter an L filter is used as a grid filter. The cascade inverter is controlled by the mean of RT-Lab. The predictive current regulator and one-phase synchronous reference frame PLL are designed with help of Rapid Control Prototyping. The proposed control method uses a discrete model of the system to predict behavior of the system for each of 15 voltage levels of inverter output voltage. Verification by simulation and on a laboratory model is described.

Key words: Cascade inverter, Predictive current control, RT-Lab, Synchronous frame PLL

Strujno prediktivno upravljanje mrežnim H-mosnim izmjenjivačem. U ovom radu prikazan je kaskadni mrežni izmjenjivač u H-mostu sa strujnim prediktivnim upravljanjem. Predloženi 15-razinski kaskadni izmjenjivač sadrži tri H-mosna izmjenjivača s odvojenim DC izvorima. Na izlazu kaskadnog izmjenjivača dodan je induktivni mrežni filter. Kaskadni izmjenjivač upravlja se korištenjem *RT-Lab* programskog okruženja. Strujni prediktivni regulator i jednofazni PLL poravnat sa sinkronim koordinatnim sustavom dizajnirani su uz pomoć *Rapid Control Prototyping* metode. Predložena metoda upravljanja koristi diskretni model sustava za predikciju ponašanja sustava u svakom od 15 naponskih razina izlaznog napona izmjenjivača. Upravljanje je provjereno na simulacijskom modelu sustava i laboratorijskom postavu.

Ključne riječi: kaskadni izmjenjivač, strujno prediktivno upravljanje, RT-Lab, PLL u sinkronom koordinatnom sustavu

1 INTRODUCTION

The solar energy and especially photovoltaics is one of the fastest growing industries in the world. There is a demand for high quality electrical energy and thus the use of photovoltaics is almost impossible without modern power electronics. If we omit the simplest PV battery charger there always has to be certain power conditioning unit (PCU) between the PV generator and the load whether to maximize the energy yield or to change certain qualities of electrical energy. Whether it is a stand-alone PV electrical generator or a grid-connected system there is a demand to change the DC voltage to the AC voltage, to maximize the energy yield and to monitor the whole system. This is done by the mean of a PV inverter. There are several types of PV inverters according to the topology. However, there is little experimentation with alternative inverter topologies [1]. The most widely used topology employs full-bridge (H-bridge) voltage source inverter. This paper describes the cascade H-bridge inverter which can be used for photovoltaic applications.

The cascade H-bridge inverter is an alternative to the single H-bridge inverter in photovoltaic systems. Its advantages over the single H-bridge inverter are lower THDi of the grid current and THDu of the output voltage, requirements of smaller filters, ability to transfer more power and smaller du/dt stresses. There is a need to increase the lifetime of photovoltaic inverters as well as their reliability. High voltage stresses decrease the lifetime of many electrical components [2]. Lower du/dt stresses of components in multilevel H-bridge inverter can help to meet these needs.

The lifetime of PV generators is in the range of 25 years and their reliability is high. However, the lifetime of typical inverter is in the range of 5 – 10 years (in 2006) [1]. It means that the inverter needs to be replaced several times during the lifetime of the PV generator. According to several biggest PV inverter producers, the PV inverter lifetime of 20 years cannot be achieved (mainly due to poor reliability of capacitors) and the price of the inverter is more

important than its lifetime. On the other hand, the cost reduction and the reliability increasing can be achieved by using new topologies of PV inverters [1].

The topologies of utility scale PV inverters are moving towards multilevel structures mainly because of smaller filtering components and better harmonic spectra [3]. Multilevel inverters are well suited for use with photovoltaics due to ease of creation separated DC sources.

Progress in the field of photovoltaics and increasing penetration of grid-tied distributed renewable energy sources leads to potential problems with those power sources into the grid. Small grid connected PV systems are usually connected to the low voltage grid. In Germany, which has more than 20 GW of grid connected PV systems installed, is approx. 80% of installed power fed to the low voltage grid [12].

Such a large power supplied from renewable energy sources can significantly influence the grid, similar to wind farms [13]. The PV plants are thus moving from pure grid feeders to sources at least partially responsible for power quality.

2 CASCADE H-BRIDGE INVERTER

2.1 Multilevel Converter Topologies

Multilevel inverters have been used for many years in high-voltage, high-power applications. Their capability to divide the net voltage and power between several smaller cells and to produce higher quality voltage and current were the reason for their spreading in these areas. The most widely used topologies in industry are cascade inverter, diode-clamped NPC inverter and capacitor-clamped (flying capacitor) NPC inverter.

Multilevel inverters usually need several separated DC sources which is one of the biggest problems they have. However, in the area of photovoltaics, the separated DC sources with galvanic isolation are not a problem. A DC/DC converter such as in [10, 11] can be used. Even though, not all above-mentioned multilevel topologies are suitable for PV inverter. The diode-clamped NPC inverter has a complicated active power control and the capacitor-clamped NPC inverter has low efficiency when it has to transfer the active power [4].

In [2] the cascade H-bridge inverter with several isolation transformers is suggested as a suitable inverter topology for the PV inverter. This solution brings problems with isolation transformers which are bulky and expensive. Cascade H-bridge inverter with separated DC sources in multistring topology which is well suited for small photovoltaic installations.

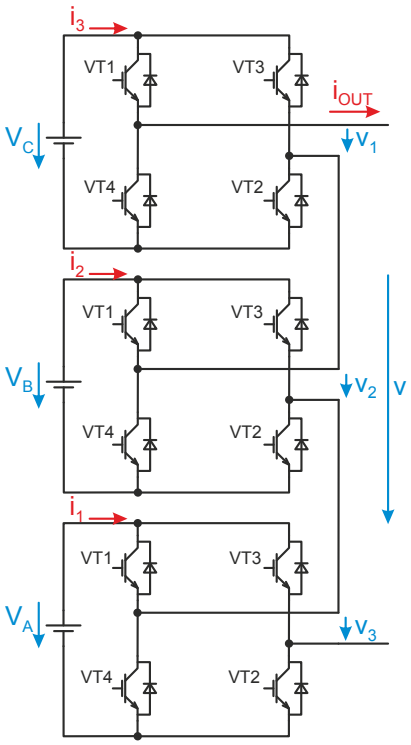

Fig. 1. Single-phase cascade H-bridge inverter with three separated DC sources ($U_A = 240$ V, $U_B = 120$ V, and $U_C = 60$ V), capable of creating 15 voltage levels at its output

2.2 Cascade H-bridge Inverter

A single-phase structure of a general 7-level cascade H-bridge inverter is shown in Fig. 1. The number of output phase voltage levels n is defined by:

$$n = 2d + 1, \tag{1}$$

where d is the number of separated DC sources.

However, in order to reduce THD of the output voltage, it is possible to create more voltage levels at the output of the cascade inverter as defined by (1) but with the same number of DC sources. Each H-bridge inverter can create positive, negative or zero voltage on its output with magnitude equal to the DC source voltage. Thus there are 15 possible combinations for the cascade H-bridge inverter with 3 separated DC sources. The example of the output voltage for DC supply voltages of 40, 20 and 10 V of three separated DC sources is shown in Fig. 2.

The measured partial voltages at the output of each H-bridge inverter are shown in Fig. 3.

It can be clearly seen that each H-bridge inverter is switching with different frequency, which is increasing as the voltage of the H-bridge inverter is decreasing. There is

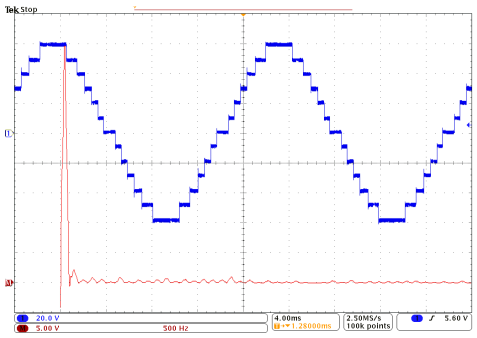

Fig. 2. Measured output voltage of 15-level (3 DC sources: $U_A = 40$ V, $U_B = 20$ V, $U_C = 10$ V) cascade H-bridge inverter with voltage control ($m_a = 0.8$, $m_f = 2$, $U_{RMS} = 42$ V, THDu= 9%)

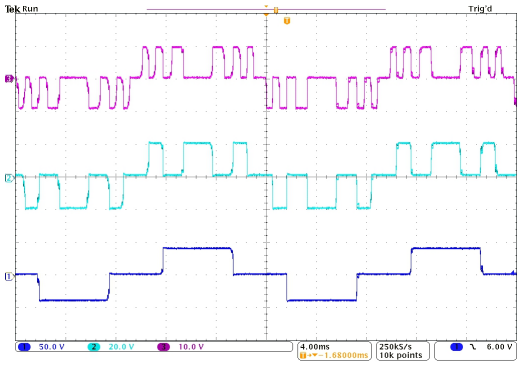

Fig. 3. Measured partial output voltages u_1, u_2, u_3 of the cascaded H-bridge inverter (amplitudes: 40, 20 and 10V), $m_a = 0.8$, $m_f = 2$

discontinuous power transfer at the output of each bridge cell.

3 CURRENT CONTROL TECHNIQUE

If we consider the DC/DC converter at the inverter input this DC/DC converter acts as a voltage source. Thus the inverter must be a voltage source inverter (VSI). There are two main control strategies for VSI: the voltage control (VCVSI) and the current control (CCVSI). They vary in the way they control the power flow. The VCVSI uses the control of the decoupling inductor voltage to control the power flow and the CCVSI uses the decoupling inductor current to control the power flow. The CCVSI is faster, can control active and reactive power flow independently but cannot provide the voltage support to the load, cannot operate without the grid. The CCVSI can be used for power factor correction due to the fact, that it can control the reactive power independently from the active power [5]. The CCVSI has also a limited short circuit current compared to the VCVSI.

The cascade inverter controller (Fig. 4) consists of several parts: grid measurements, PLL, reference current generator, predictive current controller and coder.

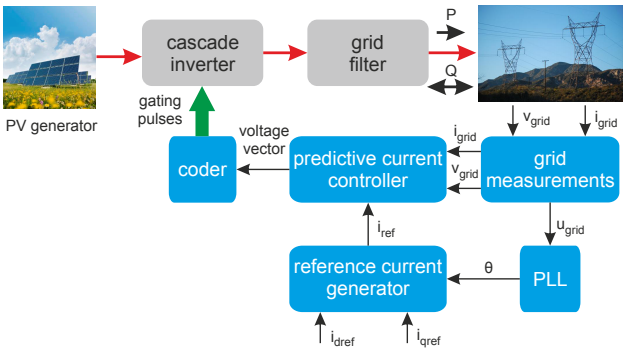

Fig. 4. Current control of grid connected PV system

3.1 Predictive Current Controller

There are various control techniques to control the output of the inverter. When using the PWM control there is a need to linearise the model of the inverter and this control technique can lead to cascade regulation structure which has slow response time. The predictive control offers the possibility to control the inverter output current and voltage with high dynamics without the need to face the problem of non-linear nature of semiconductor power converters [6].

Predictive control techniques can be divided into three main categories: hysteresis based, trajectory based and model based predictive control. For hysteresis predictive control there is defined boundary region in which the regulator tries to keep the controlled variable. The trajectory based predictive control tries to force the controlled variable to follow the pre-calculated trajectory. The model based predictive control uses the model of the system to predict the future state of the system and thus to optimize the controlled variable [6].

In [7], authors use trajectory based predictive control for current control of three-level diode-clamped NPC inverter. This control technique has been adapted to the proposed 15-level cascade H-bridge inverter. This control technique can be broadly classified as trajectory based.

The basic principle of used predictive control technique is that the cascade H-bridge inverter can create only limited number of voltage levels at its output.

The variable of interest is the current supplied to the grid I. This current is influenced by the inverter voltage V. The goal is to predict the behaviour of the load current I for each possible voltage vector generated by the inverter.

The system shown in Fig. 5 can be described by:

$$v = Ri + L\frac{di}{dt} + e. \tag{2}$$

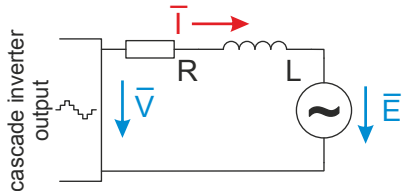

Fig. 5. The L filter between the inverter output and the grid used to decouple the output voltage and the grid and to filter higher harmonics

The prediction of the load current is based on the discrete model, which can be easily implemented by computer. The derivative in (2) can be replaced by its discrete approximation (T_S is the sampling time):

$$\frac{di}{dt} \approx \frac{i\left(k+1\right)-i\left(k\right)}{T_S}. \tag{3}$$

By replacing (3) in (2), the discrete model of the system is obtained:

$$v\left(k\right)=Ri\left(k\right)+L\frac{i\left(k+1\right)-i\left(k\right)}{T_S}+e\left(k\right). \tag{4}$$

From (4), the future value of the load current predicted form the model of thy system is:

$$i\left(k+1\right)=\frac{T_S}{L}\left(v\left(k\right)-e\left(k\right)\right)+i\left(k\right)\left(1-\frac{RT_S}{L}\right). \tag{5}$$

The (5) is used to predict the future value of the load current. For the trajectory based predictive control there is a need to create the trajectory which will be followed by the controlled variable. However, the future value of the reference current $i^*(k+1)$ is unknown. In order to determine the next value of the reference current, in [7] they use Lagrange quadratic extrapolation which uses Lagrange polynomials that are polynomials of the least degree that at each point assume the corresponding value of the function.

$$i^*\left(k+1\right)=3i^*\left(k\right)-3i^*\left(k-1\right)+i^*\left(k-2\right). \tag{6}$$

For predictive control, there is a need to create the cost function which will be evaluated in each sampling time and will define the behaviour of the system. The cost function can determine the quality of control process. It can be chosen so that it can minimize the switching frequency or the higher order harmonics. The function can be chosen as a filter to remove certain harmonics and so on [6].

The cost function was chosen as difference between the desired and real value of the current supplied to the grid:

$$z\left(k\right)=\left|i^*\left(k+1\right)-i\left(k+1\right)\right|. \tag{7}$$

The cost function (7) is evaluated for each of 15 voltage vectors that the cascade H-bridge inverter can create at its output and the voltage vector V that minimizes the cost function (7) is chosen and applied at the inverter output. The example of cost function evaluation in time is shown in Fig. 7. Each voltage level generates one value of the cost function in time. The voltage level, that is closest to zero is chosen and is hold at the inverter output for the whole sampling time. From Fig. 6, it can be seen that the sampling time is not directly related to the switching frequency as the same voltage level can be applied for more than one sampling time. This brings the possibility to limit the switching frequency but it brings decrease of the quality of load current tracking ability.

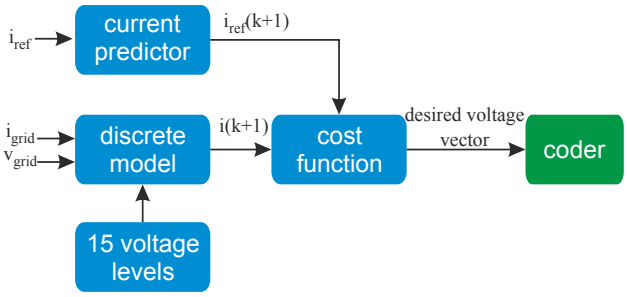

Fig. 6. The predictive current controller

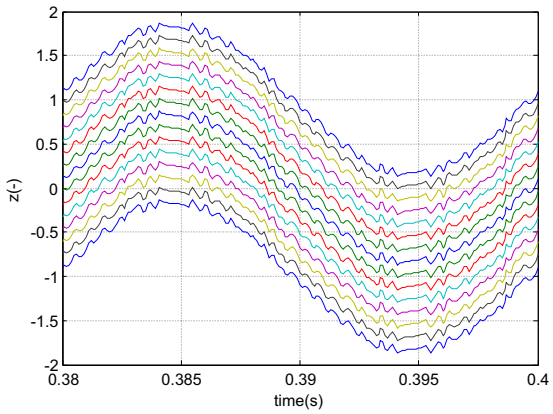

Fig. 7. The cost function (the absolute value is omitted) evaluation in time ($U_A = 240$ V, $U_B = 120$ V, $U_C = 60$ V, $T_S = 200$ μs, $R = 1\ \Omega$, $L = 6$ mH)

The current controller structure is shown in Fig. 6. The inputs are grid voltage and current and the reference current from the reference current regulator. The discrete model of the system is calculated for each voltage vector and the voltage vector that minimise the cost function is chosen. The output of the predictive current regulator is the desired voltage vector which is fed to the coder. The coder is responsible for the control of switching states of

H-bridges to create the desired voltage level at the inverter output.

3.2 Phase Locked Loop

The PLL (Phase Locked Loop) is a mean how to synchronize the grid connected system to the grid voltage. The synchronization is needed for power factor control. PLL synchronization techniques can be divided into two groups: open loop and closed loop. The most widely used technique in three-phase system is synchronous reference frame PLL (SF-PLL). The SF-PLL has good performance with the grid which is not highly distorted [8].

The SF-PLL is based on direct Clark transformation of the three-phase system into two-phase system and the subsequent Park transformation into synchronous reference frame. Thus two voltages v_d and v_q are produced. One of these voltages is by a mean of PI controller set to zero which results in the reference being locked to the grid. The output from the PLL is a phase angle which is used to generate the reference three-phase currents through reverse Park transformation ($dq \rightarrow \alpha\beta$) and subsequent reverse Clark transformation ($\alpha\beta \rightarrow abc$).

The SF-PLL can be used for one-phase systems as well. However, it is not possible to use the direct Clark transformation because only one voltage is presented. The solution is to create artificial two-phase system based on the one-phase grid voltage [8, 9].

The property of the stationary reference frame is that two voltages v_α and v_β are orthogonal. If the grid voltage corresponds to the v_β voltage, than the v_α can be created as follows:

$$\begin{bmatrix} v_\alpha \\ v_\beta \end{bmatrix} = \begin{bmatrix} v_{grid}\,(\omega t - \pi/2) \\ v_{grid}\,(\omega t) \end{bmatrix} = \begin{bmatrix} V_m \sin(\omega t - \pi/2) \\ V_m \sin(\omega t) \end{bmatrix} \cong \begin{bmatrix} -V_m \cos(\omega t) \\ V_m \sin(\omega t) \end{bmatrix}. \tag{8}$$

There are several possibilities how to create the 90 degrees phase shift of the grid voltage to produce the v_α voltage (e.g. storage elements, filters). One of them is to use second-order low-pass filter [8, 9]. Based on the comparison in [8] the best performance is achieved by PLL with second order filter artificial voltage generator and SF-PLL. When the input voltage v_{grid} passes through the second-order low-pass filter, where the damping ratio $\zeta = 1/\sqrt{2}$, the undamped natural frequency ω_n has the same value as the estimated frequency, a signal with a phase-angle difference of $\pi/2$ and amplitude of $V_m/\sqrt{2}$ is obtained [8]:

$$u_\alpha = -\sqrt{2}\frac{V_m}{\sqrt{2}} \sin\left(\omega t - \frac{\pi}{2}\right) = V_m \cos(\omega t)\,. \tag{9}$$

The one-phase synchronous reference frame PLL is shown in Fig. 8. The input is a grid voltage which passes through a low-pass filter. The amplitude and phase of that filter is compensated, as suggested in [8].

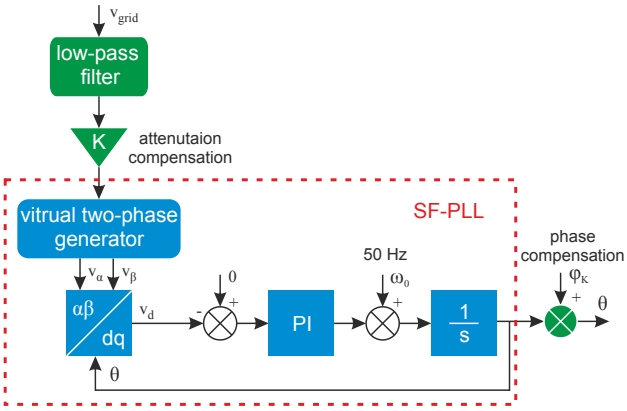

Fig. 8. One-phase synchronous reference frame PLL

The PLL is implemented as discrete model and filters coefficients are obtained by Tustin transformation.

3.3 Reference Current Generator

The reference current generator (Fig. 9) consists simply of direct Park transformation. The i_α is set as reference current i_{ref} for current regulator.

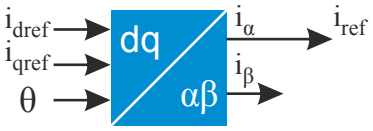

Fig. 9. Reference current generator

The inputs to the reference current generator are dq components of required grid current. These components are connected to active and reactive power delivered to the grid. There is a need to create dq power controller to control required components of the grid current.

4 SIMULATION RESULTS

The proposed controller was at fist simulated in MATALB/Simulink. This environment was chosen due to its ability to easily transfer the designed model to RT-Lab, which was used for real time simulation of designed controller and Rapid Control Prototyping. The MATLAB/Simulink model of a predictive current controller used for simulation is shown in Fig. 10.

Simulations were done for the same operating conditions as the real laboratory setup has. For the simulation and for the real measurements, the system parameters

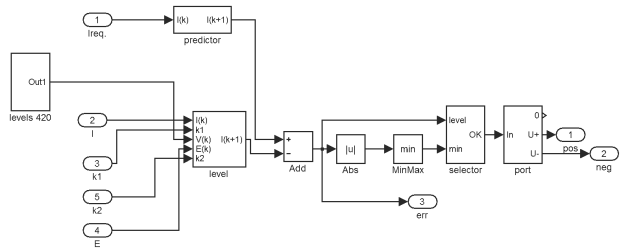

Fig. 10. The Simulink model of used current predictive regulator

were: $R = 5\ \Omega$, $L = 7$ mH, $T_S = 100\ \mu$s, $U_A = 40$ V, $U_B = 20$ V, $U_C = 10$ V, the grid voltage $E = \sim 35$ V, 50 Hz.

The basic capability of the controller that needs to be verified is the ability to track the load current and the lock capability and speed of the PLL. Comparison between the desired and the real value of the load current is shown in Fig. 11. The total harmonic distortion of load current THDi is 2.5%. The designed current controller has the capability to follow the reference current generated by the reference current generator as can be seen in Fig. 11.

The sampling time should be chosen with respect to the load parameters, the required total harmonic distortion of current THDi and total harmonic distortion of voltage THDu and is limited by computing speed of used real-time system.

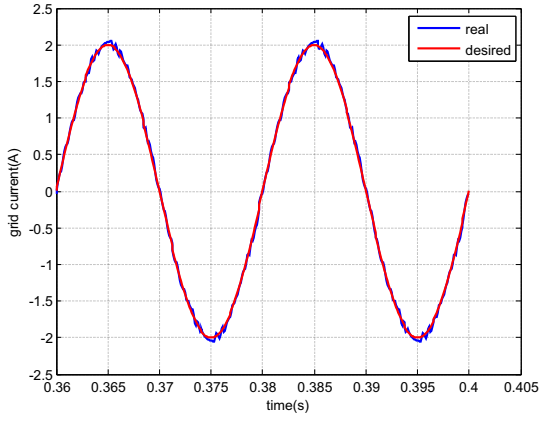

Fig. 11. The simulation of tracking ability for load current and its changes ($U_A = 40$ V, $U_B = 20$ V, $U_C = 10$ V, $E = \sim 35$ V, 50 Hz, $T_S = 100\ \mu$s, $R = 5\ \Omega$, $L = 7$ mH, $i_{dref} = 2$ A, $i_{qref} = 0$ A)

Performance of the PLL was verified by observing the time that is needed for the grid current to lock to the grid voltage as shown in Fig. 12. The PLL was locked after 15 ms. The grid voltage and current are in phase due to required value of grid current dq components (the q component was set to zero, thus there is no phase shift).

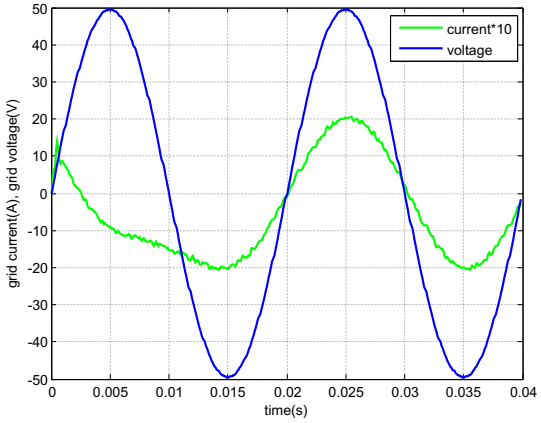

Fig. 12. The performance of the PLL locking speed ($U_A = 40$ V, $U_B = 20$ V, $U_C = 10$ V, $E = \sim 35$ V, 50 Hz, $T_S = 100\ \mu$s, $R = 5\ \Omega$, $L = 7$ mH, $i_{dref} = 2$ A, $i_{qref} = 0$ A)

The values at the inverter output are shown in Fig. 13. The change in the inverter voltage is at most every 100 μs and is defined by the sampling time.

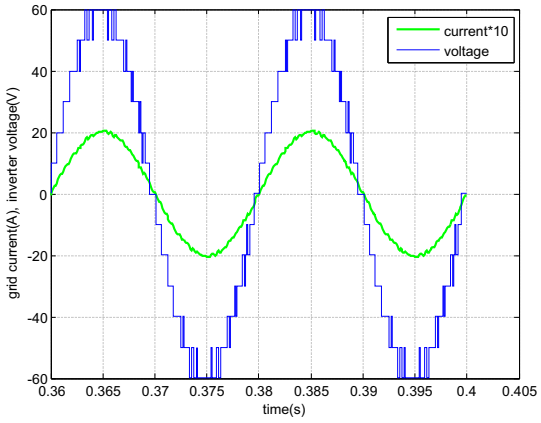

Fig. 13. The cascade inverter output ($U_A = 40$ V, $U_B = 20$ V, $U_C = 10$ V, $E = \sim 35$ V, 50 Hz, $T_S = 100\ \mu$s, $R = 5\ \Omega$, $L = 7$ mH, $i_{dref} = 2$ A, $i_{qref} = 0$ A)

5 REAL SYSTEM SETUP

The after mentioned current control technique was used to control the laboratory model of a 15-level (three DC sources: 40V, 20V and 10V) cascade inverter with L filter connected to $\sim$ 35 V/50 Hz. The control circuit was designed with the help of Rapid Control Prototyping (RCP) and RT-Lab. The biggest advantage of this solution is that with the help of RT-Lab the Simulink model can be run in real time.

When using RCP, which is a part of the Hardware in the Loop (HIL) simulation, the controller is simulated on a computer in real time and is connected to a real plant (Fig. 14). This technique can easily verify the controller design. The plant is the 15-level cascade inverter with 3 separated DC sources in this case. Simulink was used to create a program scheme of the controller and RT-Lab was used to simulate the controller in real time.

The connection between the real-time system and a real hardware is accomplished by a mean of DAQ card with digital and analogue inputs/outputs. Texas Instruments 6025E DAQ card is used. The dead time needed to prevent short circuit in H-bridge leg is realized by the hardware IGBT driver circuit. The current regulator is sampled with sample time $T_S = 100$ μs. With current system configuration the sample time can be set as low as 50 μs.

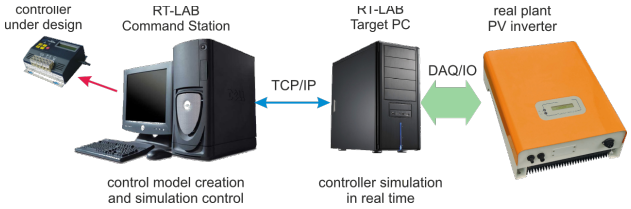

Fig. 14. Interconnection of simulated regulator and a real plant (AC motor in this case for illustrative purpose) using RT-Lab during RCP procedure

6 EXPERIMENTAL RESULTS

With measurements on the 15-level cascade H-bridge inverter, the tracking capability of the load current and the power factor control were verified. For measurements, the system parameters were set to: $R = 5\ \Omega$, $L = 7$ mH, $T_S = 100$ μs, $U_A = 40$ V, $U_B = 20$ V, $U_C = 10$ V (voltage sources). The inverter was connected to the one-phase grid ~ 35 V/50 Hz.

The reference current was set as $i_{dref} = 2$ A, $i_{qref} = 0$ A, thus the power factor should be 1. The active and reactive power supplied to the grid, as well as phase shift between grid voltage and current, was measured by power analyzer. The real phase shift was 2 degrees into inductive region (PF of 0.9996 inductive). Thus the reactive power was consumed by the inverter (Fig. 15). This error can be eliminated by creating a bias in i_{qref}.

7 CONCLUSION

In this paper the 15-level grid-tied cascade H-bridge inverter with predictive current control technique is presented. From the simulation and experimental results can be concluded that the proposed current regulator and PLL

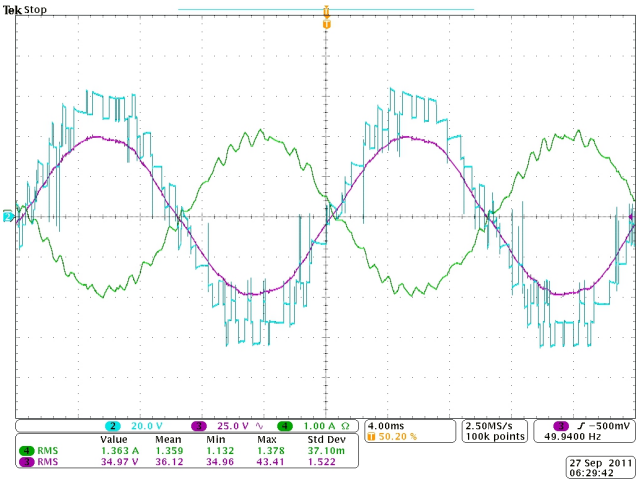

Fig. 15. Output current of cascade inverter with current control: CH2: inverter voltage, CH3: grid voltage, CH4: grid current ($T_S = 100$ μs, $R = 5\ \Omega$, $L = 7$ mH, $U_A = 40$ V, $U_B = 20$ V, $U_C = 10$ V, THDi = 4%, $P = 50$ W, $Q = -1.3$ W, $\varphi = 2°$ inductive, $i_{dref} = 2$ A, $i_{qref} = 0$ A)

synchronisation work properly. Only some aspects are presented here and many problems are still to be solved. Future research will be oriented towards connection to the PV generator and design of MPPT (Maximum Power Point Tracking) control, which is essential for a PV inverter. Also the problem with unloaded DC sources (partial PV generators in real system) will be solved. Replacement of the simple L filter with a LCL filter is next challenge. The used cost function is very simple and by creating more sophisticated cost function, the control technique will be improved. The difference between presented simulation results and measurements is caused by inaccuracy of sensors and L filter parameters. However, the work shows promising results and by using computer control and RT-Lab, the controller can be easily modified.

ACKNOWLEDGMENT

This work was supported by the Slovak Research and Development Agency under the contract No. APVV-0185-10. The authors also wish to thank for the support to the R&D operational program Centre of excellence of power electronics systems and materials for their components No. OPVaV-2008/2.1/01-SORO, ITMS 26220120003 and No. OPVaV-2009/2.1/02-SORO, ITMS 26220120046 funded by European Regional Development Fund (ERDF).

REFERENCES

[1] National Renewable Energy Laboratory, "A Review of PV Inverter Technology Cost and Performance Projections", 2006.

[2] S. Daher, J. Schmid, F. Antunes, "Current Demand of High Performance Inverters for Renewable Energy Systems", European Conference on Power Electronics and Applications - EPE, 2007.

[3] Yaosuo Xue, K.C. Divya, G. Griepentrog, M. Liviu, S. Suresh, M. Manjrekar, "Towards Next Generation Photovoltaic Inverters", IEEE, 2011.

[4] S. Khomfoi, L. M. Tolbert: Multilevel Power Converters, chapter from H.Rashid: Power Electronics Handbook, 2nd edition, Elsevier, 2007, ISBN10: 0-12-088479-8, pp. 451 – 482.

[5] S. H. Ko, S. R. Lee, H. Dehbonei, Ch. Nayar, "A Comparative Study of the Voltage Controlled and Current Controlled Voltage Source Inverter for the Distributed Generation System" [Online]. AUPEC 2005, 2005.

[6] R. Kennel, "Predictive Control of Inverter Supplied Electrical Drives", in Power Electronics Specialists Conference, 2000. PESC 2000 IEEE 31st Annual, 2000, pp. 761 - 766 vol.2.

[7] G. S. Perantzakis, F. H. Xepaps,S. A. Papathanassiou, S. N. Manias, "A Predictive Current Control Technique for Three-Level NPC Voltage Source Inverter", in Power Electronics Specialists Conference, 2005. PESC '05. IEEE 36th, 2005, pp. 1241 – 1246.

[8] J.-W. Choi, Y.-K. Kim, H.-G. Kim, "Digital PLL control for single-phase photovoltaic system", Electric Power Applications, IEE Proceedings, 2006.

[9] B. Meersman, J. De Kooning, T. Vandoorn, L. Degroote, B. Renders, L. Vandevelde, "Overview of PLL methods for distributed generation units", UPEC 2010, 2010.

[10] J,. Hamar, I. Nagy, P. Stumpf, H. Ohsaki, E. Masada, "New Dual Channel Quasi Resonant DC-DC Converter Toplogies for Distributed Energy Utilization", EPE-PEMC 2008, 2008, pp. 1778-1784.

[11] E. Eotvos, J. Dudrik, T. Beres, "Resonant LLC converter for photovoltaics", In: EDPE 2011 : 17th International Conference on Electrical Drives and Power Electronics : proceedings :, Stará Lesná, High Tatras, Slovakia. Košice, 2011, 102-105. - ISBN 978-80-553-0734-3.

[12] SMA, "Technology Compendium 3.3 – PV Grid Integration", 2011.

[13] V. Spudić, M. Jelavić, M. Baotić, "Wind Turbine Power References in Coordinated Control of Wind Farms", Automatika - Journal for Control, Measurement, Electronics, Computing and Communications, Vol. 52, No. 2, 2011, pp. 82 - 94.

Marek Pástor was born in Košice (Slovakia) in 1985. He received his master degree in electrical engineering in 2010. He is currently working towards a PhD. degree at Dept. of Electrical Engineering and Mechatronics, Technical University of Košice, Slovakia. His interest is in the area of power electronics.

Jaroslav Dudrik received the M.S. and Ph.D. degrees in electrical engineering from the Technical University of Košice, Slovakia, in 1976 and 1987. He is currently full professor of Electrical Engineering at the Department of Electrical and Mechatronic Engineering, Technical University of Košice, where he is engaged in teaching and research. His primary interest is power electronics. His field of research includes DC-to-DC converters, high power soft switching converters, converters for renewable energy sources and control theory of converters.

AUTHORS' ADDRESSES

Marek Pástor, M.Sc.
Prof. Jaroslav Dudrik, Ph.D.
Department of Electrical Engineering and Mechatronics,
Faculty of Electrical Engineering and Informatics,
Technical University of Košice,
Letná 9, SK-042 00, Košice, Slovakia
email: marek.pastor@tuke.sk,jaroslav.dudrik@tuke.sk

Received: 2012-01-30
Accepted: 2012-06-21